Glycobiology vol. 15 no. 5 pp. 489–500, 2005
doi:10.1093/glycob/cwi034
Advance Access publication on December 22, 2004

Kinetic analysis of a Golgi UDP-GlcNAc:polypeptide-Thr/Ser *N*-acetyl-α-glucosaminyltransferase from *Dictyostelium*

Altan Ercan and Christopher M. West[1]

Department of Biochemistry and Molecular Biology, Oklahoma Center for Medical Glycobiology, University of Oklahoma Health Sciences Center, 940 Stanton L. Young Blvd., BMSB 937, Oklahoma City, OK 73104

Received on August 29, 2004; revised on November 27, 2004; accepted on November 29, 2004

Mucin-type *O*-glycosylation in *Dictyostelium* is initiated in the Golgi by a UDP-GlcNAc:polypeptide-Thr/Ser *N*-acetyl-α-glucosaminyltransferase (*Dd*-pp αGlcNAcT2) whose sequence is distantly related to the sequences of animal polypeptide-Thr/Ser *N*-acetyl-α-galactosaminyltransferases, such as murine *Mm*-pp αGalNAcT1. To evaluate the significance of this similarity, highly purified *Dd*-pp αGlcNAcT2 was assayed using synthetic peptides derived from known substrates. *Dd*-pp αGlcNAcT2 strongly prefers UDP-GlcNAc over UDP-GalNAc, preferentially modifies the central region of the peptide, and modifies Ser in addition to Thr residues. Initial velocity measurements performed over a matrix of UDP-GlcNAc donor and peptide acceptor concentrations indicate that the substrates bind to the enzyme in ordered fashion before the chemical conversion. Substrate inhibition exerted by a second peptide, and the pattern of product inhibition exerted by UDP, suggest that UDP-GlcNAc binds first and the peptide binds second, consistent with data reported for *Mm*-pp αGalNAcT1. Two selective competitive inhibitors of *Mm*-pp αGalNAcT1, retrieved from a screen of neutral-charge uridine derivatives, also inhibit *Dd*-pp αGlcNAcT1 competitively with only slightly less efficacy. Inhibition is specific for *Dd*-pp αGlcNAcT2 relative to two other *Dictyostelium* retaining glycosyltransferases. These data support a phylogenetic model in which the αGlcNAcT function in unicellular eukaryotes converted to an αGalNAcT function in the metazoan ortholog while conserving a similar reaction mechanism and active site architecture.

Key words: evolution/inhibitor/mucin type/*O*-glycosylation/reaction mechanism

Introduction

Biochemical and genetic studies show that mucin-type *O*-linked glycosylation contributes multiple developmental (Schwientek *et al*., 2002; Ten Hagen and Tran, 2002) and homeostatic functions in animals. Mucin-type *O*-glycans are important for cell–cell interactions, such as sperm–egg contact and leukocyte homing, protein trafficking, protection against proteolytic digestion, and ligands or decoys for parasites (Varki, 1993; Varki *et al*., 1999). Mucin-type traditionally refers to *O*-glycans that are attached via GalNAc in α-linkage to the hydroxyl side chain of Thr or Ser residues of proteins in the animal cell secretory pathway (Spiro, 2002). Target residues tend to be clustered in identical or degenerate hydrophilic amino acid repeats of proteins (Perez-Vilar and Hill, 1999) but can also be solitary. The GalNAc substituent is usually extended by specific sugar sequences that include Gal and GlcNAc and are often capped with anionic moieties, typically sialic acid or sulfate. A unicellular taxon, the apicomplexans, also expresses the αGalNAc class of mucin-type *O*-glycans (O'Connor *et al*., 2003).

Two unicellular eukaryotes, *Trypanosoma cruzi* and *Dictyostelium discoideum*, have *O*-glycans that are attached by αGlcNAc instead of αGalNAc (Jung *et al*., 1998; Previato *et al*., 1998; Zachara *et al*., 1996). These also tend to be clustered in hydrophilic amino acid repeats of secretory or cell surface proteins. In trypanosomes, the anionic substituents are host-derived sialic acid, whereas in *Dictyostelium* they are typically phosphomonoesters or -diesters. Though the glycan structures vary from those of animals, the microbial αGlcNAc-linked glycans are often referred to as mucin-type. In *Dictyostelium*, these *O*-glycans support protein stability important for cell–cell adhesion and contribute to pattern formation, cell traction during motility, and spore coat assembly (reviewed in West, 2003). For *T. cruzi*, there is evidence that mucin glycans are important for the recognition and invasion of mammalian cells, although the mechanism(s) is still unclear (Burleigh and Andrews, 1998).

Recently, a gene that encodes the polypeptide (pp) αGlcNAcT that initiates this type of *O*-glycosylation in *Dictyostelium* has been cloned and the enzyme characterized (Wang *et al*., 2003). UDP-GlcNAc:polypeptide-Thr/Ser *N*-acetyl-α-glucosaminyltransferase-2 (*Dd*-pp αGlcNAcT2) is a type 2 membrane protein that catalyzes the attachment of GlcNAc in *O*-linkage to Thr- and Ser-rich regions of secretory and glycosylphosphatidylinositol (GPI)-anchored proteins. Mutational studies suggest that *Dd*-pp αGlcNAcT2 is required for most if not all mucin-type *O*-glycosylation in the Golgi. This enzyme was initially identified owing to its distant sequence similarity to a gene that encodes a soluble, cytoplasmic pp αGlcNAcT (*Dd*-pp αGlcNAcT1), which modifies a specific 4-hydroxyproline residue on the cytoplasmic/nuclear protein Skp1 (van der Wel *et al*., 2002). The sequences of the catalytic domains of these two enzymes share key motifs with the animal pp αGalNAcTs, a family of up to 20 related enzymes in humans, which share the role of initiating mucin-type *O*-glycan formation in animals and also apicomplexans (Hagen *et al*., 2003; Wojczyk *et al*., 2003). Site-directed mutagenesis of the DxD-like DxH

[1]To whom correspondence should be addressed; e-mail: cwest2@ouhsc.edu

Downloaded from https://academic.oup.com/glycob/article-abstract/15/5/489/602562 by Abdullah Gul Universitesi user on 02 April 2020

motif of *Dd*-pp αGlcNAcT1 has similar inactivating effects on this enzyme and *Mm*-pp αGalNAcT1 (Hagen *et al*., 1999; van der Wel *et al*., 2002). All three enzymes require divalent cations and retain the configuration of the transferred sugar. These observations support a similarity initially suggested by the sequence alignments. Bioinformatics studies suggest that the secretory pathways of many unicellular eukaryotes, including trypanosomatids, diatoms, and oomycetes, possess *Dd*-pp αGlcNAcT2-like enzyme gene sequences (West *et al*., 2004). A phylogenetic analysis of these sequences suggests that the pp αGlcNAcTs and pp αGalNAcTs share a common evolutionary ancestor, possibly of the pp αGlcNAcT type (West *et al*., 2004), which might have subsequently diversified with the appearance of a UDP-GalNAc epimerase to provide a new donor substrate (Roper and Ferguson, 2003).

The evolutionary model predicts mechanistic similarities between mammalian pp αGalNAcTs and unicellular pp αGlcNAcTs, which are examined here. Kinetic analyses suggest that *Dd*-pp αGlcNAcT2 utilizes an ordered bi bi reaction mechanism, which is not inconsistent with data reported for *Mm*-pp αGalNAcT1 (Wragg *et al*., 1995, 1997). Recently, a 1338-member uridine conjugate library, formed by condensation of uridine derivitized at its 5′-position with aminoxy or hydrazide moieties with heterocyclic aldehydes, was synthesized and used to identify inhibitors of UDP-Gal epimerase (Winans and Bertozzi, 2002). A subsequent screen yielded two different compounds, consisting of trihydroxybenzene linked to uridine via either an aminoxy or hydrazide bridge, that selectively and competitively inhibit *Mm*-pp αGalNAcT1 in vitro (Hang *et al*., 2004). This is remarkable because they lack PO_4 moieties that coordinate with the active site divalent cation (Fritz *et al*., 2004). Other studies suggest that these neutral-charge compounds can also inhibit this enzyme in living cells. It is found here that 1-68A and 2-68A are almost as effective against *Dd*-pp αGlcNAcT2 as *Mm*-pp αGalNAcT1 but have little effect on two other retaining UDP-sugar glycosyltransferases (GTs) from *Dictyostelium*. These similarities, initially suggested by bioinformatics studies, may yield practical benefits for understanding the reaction mechanisms of these enzymes and identifying inhibitors that may target their function in vivo.

Results

Reaction characterization and substrate specificity

A soluble recombinant form of pp αGlcNAcT2, whose N-terminal cytoplasmic peptide and signal anchor domains were replaced by a cleavable signal peptide, was expressed in *Dictyostelium* and purified essentially to homogeneity from the culture medium. The acceptor substrate (SP29-peptide-1, Table I) was a synthetic 26-mer peptide consisting of the entire mucin-like domain of SP29, a GPI-anchored plasma membrane glycoprotein that is a natural substrate for pp αGlcNAcT2 in vivo (Wang *et al*., 2003). SP29-peptide-1 contains 11 Thr and 2 Ser residues. Each of these hydroxyamino acid residues is glycosylated when the peptide is expressed as a fusion protein in vivo (Zachara *et al*., 1996), and none appear to be glycosylated in a pp αGlcNAcT2-null strain (Wang *et al*., 2003), suggesting that SP29 peptide-1 is potentially a substrate for 13 different glycosylation reactions. Although there are no known acceptor substrates that are modified at a single position, pp αGlcNAcT2 may not act processively because it lacks a C-terminal GalNAc-binding domain present in the pp αGalNAcTs to which pp αGlcNAcT2 is being compared (Ten-Hagen *et al*., 2003). Because a mixture of partially and fully modified peptides were observed by matrix-assisted laser desorption ionization time-of-flight mass spectrometry analyses in a reaction with a different model peptide that was carried out further to completion (Wang *et al*., 2003), each modification may represent an independent reaction cycle of acceptor substrate binding and unbinding.

Table I. Peptide acceptor substrates

Name	Sequence
SP29-peptide-1	TVTP TVTP TVTP TPTN TPNP TPSQ TS
SP29-peptide-2	TVTP SVSP TVTP TPTN TPNP TPSQ TS
SP85-peptide-2	TYPP TQPP TQPP TYPP

The initial rates of glycosylation of SP29-peptide-1 by pp αGlcNAcT2 were determined at 0.03–0.14% conversion of the 13 possible glycosylation sites of SP29-peptide-1 and 0.35 to 1.8% conversion of UDP-GlcNAc to product. The dependence of the initial rate of glycosylation on the concentration of SP29-peptide-1 at 500 μM UDP-GlcNAc, well above its previously determined apparent K_m of 38 μM (Wang *et al*., 2003), is plotted in Figure 1A (filled circles). The data exhibit a hyperbolic relationship when fitted to Equation 1 (see *Materials and methods* for all equations), indicating that the reaction rate is first order with respect to SP29-peptide-1. The data cannot be meaningfully resolved into two kinetic components. This plot suggests an average $K_m^{SP29\text{-}peptide\text{-}1}$ of 32 ± 6.5 μM, and an average k_{cat} of 31 ± 1.3 h^{-1} for the multiple modification reactions expected. The specific activity of this preparation of αGlcNAcT2 was 8 μmole mg^{-1} min^{-1}, comparable to the value of 9 μmole mg^{-1} min^{-1} reported for a recombinant *Mm*-pp αGalNAcT1 (Wragg *et al*., 1995).

To determine which acceptor amino acid residues were modified, the peptide from a reaction containing SP29-peptide-1 was subjected to sequential automated Edman degradation. Negligible radioactivity was released until cycle 5 (Figure 1B, filled bars), the position of the third hydroxyamino acid (Thr), or the first residue of the second tetrapeptide repeat. Increasing dpm were released through the middle of the peptide followed by a progressive decline. Position T17 was favored most with 24% of the incorporation, and 75% of the incorporation occurred at five central positions (11T, 13T, 15T, 17T, and 21T). The pattern of incorporation is inconsistent with a processive reaction mechanism or simultaneous modification of the peptide via multiple enzyme–substrate complexes. The kinetic homogeneity of the reaction suggests that the enzyme–substrate complex represents a family of complexes in which the specific hydroxyamino acid at the active site is stochastically distributed around the center of the peptide. Therefore

Downloaded from https://academic.oup.com/glycob/article-abstract/15/5/489/602562 by Abdullah Gul Universitesi user on 02 April 2020

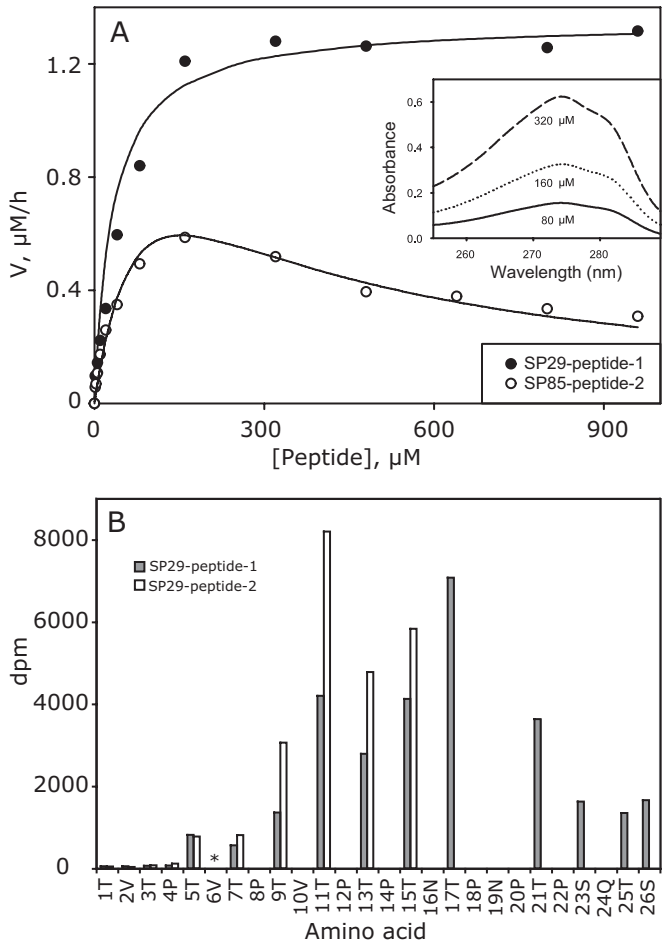


Fig. 1. Dependence of the initial rate of glycosylation by *Dd*-pp αGlcNAcT2 on acceptor substrate peptides and characterization of the reaction product. (**A**) Initial rates were determined at varying SP29-peptide-1 (filled circles) or SP85-peptide-2 (open circles) concentrations from 10 to 960 μM in the presence of 500 μM UDP-GlcNAc. The curve for SP29-peptide-1 represents the best fit of the data as a hyperbolic relationship (Equation 1), and has an R^2 value of 0.97. The curve for SP85-peptide-2 represents the model for substrate inhibition described by Equation 2, which yielded an R^2 value of 0.96 using nonlinear regression analysis. The inset shows dependence of absorbance on SP85-peptide-2 concentration (80 μM, solid line; 160 μM, dotted line; 320 μM, dashed line). (**B**) SP29-peptide-1 (filled bars) and SP29-peptide-2 (open bars) were recovered from reactions containing 240 μM peptide and subjected to automated sequential Edman degradation. Total eluate from each cycle was directly analyzed in a liquid scintillation counter. dpm values shown have been corrected for loss due to repetitive yield and asynchrony resulting from inefficient cleavage of Pro and, except for the first four residues, allocated only to positions containing Thr or Ser (*). SP29-peptide-2 was analyzed for only 15 cycles.

acceptor substrate concentration is represented as peptide rather than constituent hydroxyamino acid concentration.

pp αGlcNAcT2 appeared to modify both Thr and Ser residues of SP29-peptide-1 (Figure 1B). To verify modification of Ser, SP29-peptide-2, identical to SP29-peptide-1 except for substitution of Ser in place of Thr at positions 5 and 7, was examined in a parallel Edman degradation analysis. A similar pattern of release of radioactivity was observed from the two peptides (Figure 1B, filled versus open bars), except that the fraction of incorporation into positions of 5 and 7 relative to the other acceptor sites of the Ser-peptide was 66% that of the Thr peptide, suggesting slightly less efficient modification of Ser relative to Thr.

Substitution of UDP-[^{3}H]GalNAc for UDP-[^{3}H]GlcNAc (1 μM) resulted in only 0.7% of the rate of incorporation seen for the native substrate. Therefore, pp αGlcNAcT2 shows a strong preference for the correct C-4 epimer of the donor substrate, but further studies are required to determine the significance of the residual incorporation.

Mode of interaction of UDP-GlcNAc and peptides with Dd-*pp* α*GlcNAcT2*

To investigate enzyme mechanism, concentrations of UDP-GlcNAc and SP29-peptide-1 were separately varied from 10 to 320 μM at near saturating concentrations of the other substrate. Double reciprocal plots of the initial reaction rates with respect to either substrate concentration (Figures 2A, 3A) reveal linear trends that converge to a point left of the *y*-axis. Dependence on the concentrations of both substrates indicates that the chemical conversion requires generation of a ternary complex with pp αGlcNAcT2. The common intersection point to the left of the *y*-axis implies that the substrates bind sequentially. At unsaturating concentrations of the second substrate, the reciprocal plots are linear rather than upwardly curved, suggesting that binding is ordered rather than random (Segel, 1975). Similar data were described for *Mm*-pp αGalNAcT1 using an acceptor peptide containing a single modification site (Wragg *et al.*, 1995). These data are most consistent with an ordered bi bi reaction mechanism, in which the two substrates, UDP-GlcNAc and SP29-peptide-1, bind in prescribed order prior to chemical conversion (Cleland, 1977; Segel, 1975).

Kinetic parameters calculated from the secondary graphs (Figures 2B, 2C, 3B, 3C) yield k_{cat}, $K_m^{UDP\text{-}GlcNAc}$, $K_m^{SP29\text{-}peptide\text{-}1}$, and $K_i^{UDP\text{-}GlcNAc}$ values of 31 h^{-1}, 26 μM, 28 μM, and 190 μM, respectively. The previously reported $K_m^{UDP\text{-}GlcNAc}$ of 38 μM (Wang *et al.*, 2003) was probably an overestimate because the acceptor substrate concentration was not saturating. The $K_m^{SP29\text{-}peptide\text{-}1}$ and k_{cat} values derived from this analysis and from Figure 1A are similar.

As an independent test of kinetic mechanism, the data were replotted as a function of the reciprocal of substrate concentrations kept at a ratio at 1.0 (Figure 4). The data show a reasonable fit to the parabolic prediction of the Haldane equation (Equation 3) using a $K_i^{UDP\text{-}GlcNAc}$ value of 220 μM, similar to the value of 190 μM derived from Figures 2 and 3. This analysis provides additional support for the ordered bi bi model (Segal, 1975).

In contrast to SP29-peptide-1, another acceptor substrate, SP85-peptide-2, exhibited reduced activity at higher concentrations (Wang *et al.*, 2003). SP85-peptide-2 is derived from SP85, also a native substrate for pp αGlcNAcT2. As shown in Figure 1A (open circles), these findings are confirmed by new measurements carried out under the same conditions used to analyze SP29-peptide-1. To investigate whether lower activity at higher concentrations resulted from peptide insolubility or aggregation, three concentrations of peptides spanning the onset of inhibition (80–320 μM) were analyzed spectrophotometrically at 250–290 nm (Figure 1A, inset). Absorbance values followed Lambert-Beer's law, thus showing no indication of a change in extinction coefficient

Downloaded from https://academic.oup.com/glycob/article-abstract/15/5/489/602562 by Abdullah Gul Universitesi user on 02 April 2020

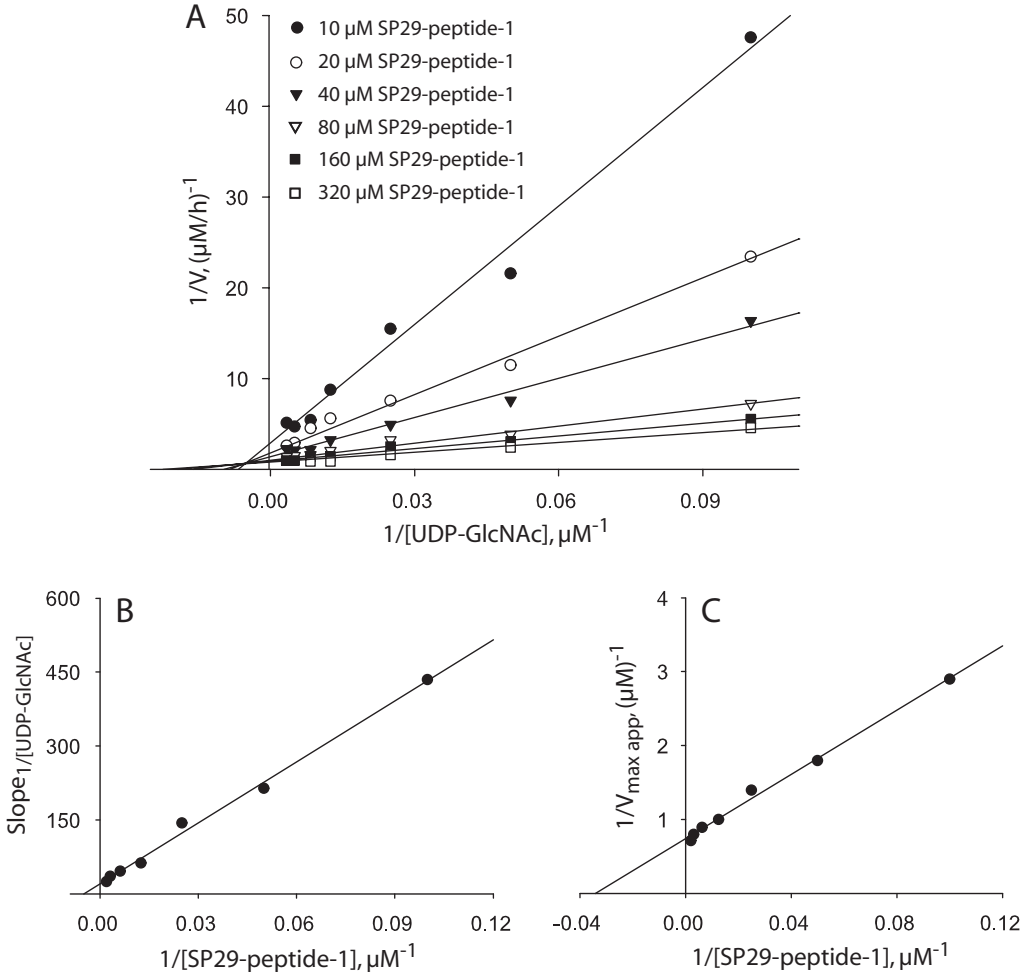


Fig. 2. Initial rate analysis of pp αGlcNAcT2 activity with respect to varying concentrations of UDP-GlcNAc at different fixed concentrations of SP29-peptide-1. (**A**) Double reciprocal plot of the data. (**B**) Plot of 1/V-axis intercepts of (**A**) versus reciprocal of [SP29-peptide-1]. (**C**) Plot of $slope_{1/[UDP\text{-}GlcNAc]}$ values from (**A**) versus reciprocal of [SP29-peptide-1]. $R^2 > 0.977$ based on nonlinear regression analysis.

or light scattering. Therefore, the lower activity of SP85-peptide-2 at high concentration most likely originates from the enzyme substrate interaction. The curve in Figure 1A (open circles) represents the best fit for the model of substrate inhibition described in Equation 2, which yields $K_m^{\text{SP85-peptide-2}}$ and $K_i^{SP85\text{-}peptide\text{-}2}$ values of 96 ± 31 μM and 250 ± 79 μM, respectively. In contrast, no inhibition was observed using SP29-peptide-1 up to the highest concentration tested, 1 mM.

SP29-peptide-1 may be a better substrate at lower concentrations because it has about threefold more hydroxyamino acids than SP85-peptide-2, which may provide greater probability of successful docking. Substrate inhibition, in which the substrate that normally binds second can bind first at high concentration and thereby interfere with the reaction, has been observed for compulsory ordered bi bi enzyme mechanisms exhibited by cellobiose phosphorylase (Kim *et al.*, 2002), (4-hydroxyphenyl)pyruvate dioxygenase (Johnson-Winters *et al.*, 2003), and *Kpn*I DNA methyltransferase (Bheemanaik *et al.*, 2003). The distinct behaviors of SP85-peptide-2 and SP29-peptide-1 may result from conformational constraints imposed by the different patterns of Pro residues in their sequences. The occurrence of two equilibrium constants for SP85-peptide-2 is most consistent with an ordered bi bi model in which binding of UDP-GlcNAc induces a conformation change that leads to a better organized binding site for SP85-peptide-2.

Inhibition of Dd-*pp* α*GlcNAcT2 by uridine-based compounds*

Nucleotides are efficient inhibitors of the pp αGalNAcTs (Wragg *et al.*, 1995) and other sugar nucleotide-dependent GTs. The dose-dependent effects of UDP, UMP, uridine, and other uridine derivatives (see below) on initial reaction velocity are described in Figure 5. The curves are best-fit models of the data based on competitive inhibition. Uridine does not inhibit at ≤ 2 mM. UMP inhibits *Dd*-pp αGlcNAcT2 competitively with respect to UDP-GlcNAc with an apparent K_i of 140 μM (values listed in Table II), based on analysis of double reciprocal plots of the data (Figure 6A). UDP is a better competitive inhibitor than UMP and has an apparent K_i of 89 μM (Figure 6B). In contrast, UDP inhibition is noncompetitive with respect to SP29-peptide-1, with an apparent K_i of 440 μM (Figures 7A, 7B). Appending GalNAc to the β-PO_4 of UDP (UDP-GalNAc is not a substrate for the reaction; see

Downloaded from https://academic.oup.com/glycob/article-abstract/15/5/489/602562 by Abdullah Gul Universitesi user on 02 April 2020

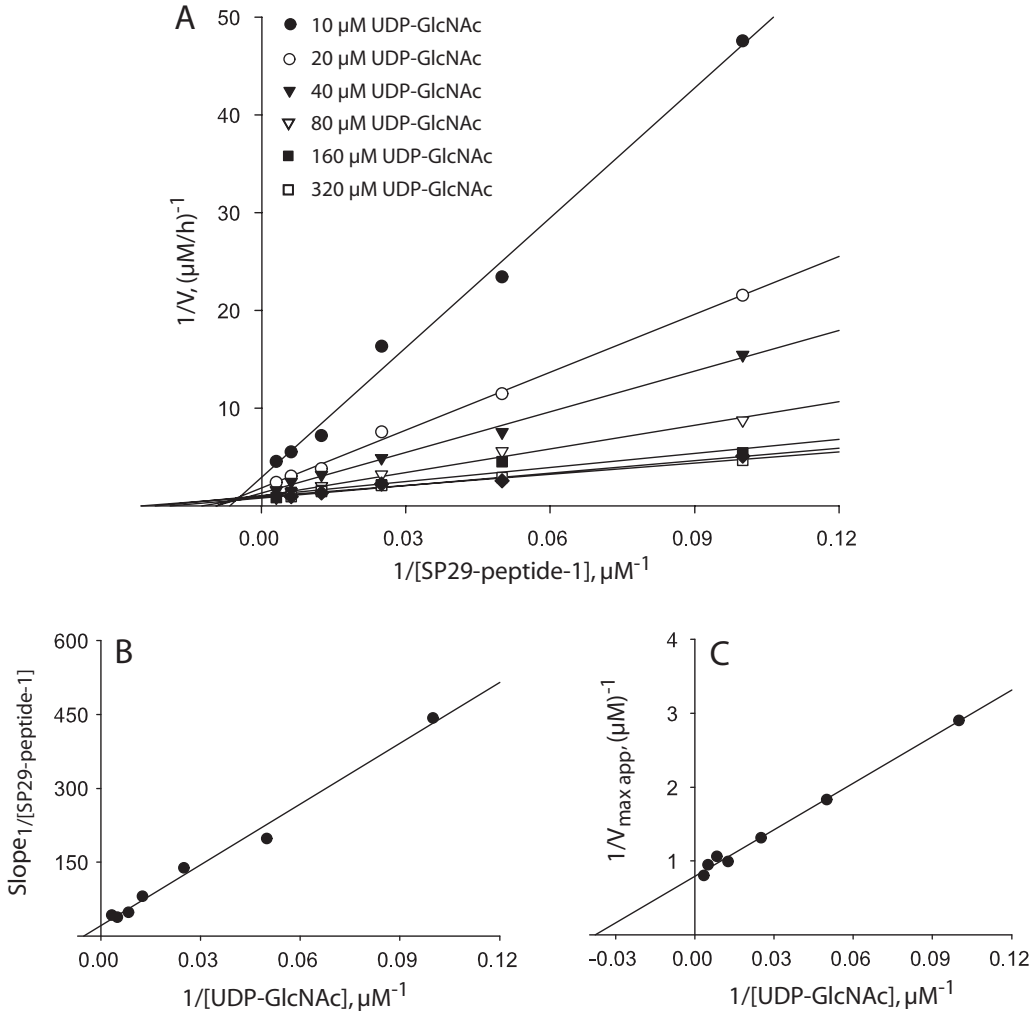


Fig. 3. Initial rate analysis of pp αGlcNAcT2 activity with respect to varying concentrations of SP29-peptide-1 at different fixed concentrations of UDP-GlcNAc. (**A**) Double reciprocal plot of the same data as in Figure 2A. (**B**) 1/V-axis intercept replot as in Figure 2B. (**C**) $Slope_{1/SP29}$ replot.

results above) increased the apparent K_i to close to the value for UMP (Table II). The differences among these compounds correlate with the greatest structural similarity of UDP to the substrate UDP-GlcNAc and to the product UDP. Competitive inhibition of UDP against the donor substrate and noncompetitive inhibition against the acceptor substrate, observed previously for recombinant *Mm*-pp αGalNAcT1 (Wragg *et al*., 1995), is most consistent with the two substrate–binding site model suggested by the kinetic studies described, in which the donor substrate binds first followed by subsequent binding of the acceptor substrate (Table IX-6 in Segel, 1975).

Compounds 1-68A and 2-68A, recently described inhibitors of *Mm*-pp αGalNAcT1 (see Introduction), are better inhibitors of pp αGlcNAcT2 than UMP and UDP (Figure 5). 1-68A and 2-68A each inhibit competitively with respect to UDP-GlcNAc (Figures 6C, 6D), with apparent K_i values of 35 and 70 μM, respectively. These compare with the 8–35 μM apparent K_i values exerted on murine pp αGalNAcTs (Hang *et al*., 2004). The trihydroxybenzene moiety, 68A, exerts much weaker inhibition with a competitive apparent K_i with respect to UDP-GlcNAc of 220 μM (Figure 6E). Therefore the conjugates appear to achieve their inhibitory potency from joining of uridine and trihydroxybenzene, proposed previously to act as a sugar mimic (Hang *et al*., 2004). 1-68A and 2-68A appear to interact with the UDP-GlcNAc binding site of pp αGlcNAcT2, because of the competitive nature of their inhibition. However, the interaction appears to be more complex than observed for UDP (Figures 7A, 7B), based on analysis of inhibition with respect to SP29-peptide-1. At low concentrations, 1-68A appears to inhibit competitively (Figures 7C, 7D), but at higher concentrations displays mixed inhibition. At low concentrations of SP29-peptide-1, high concentrations of 1-68A appear to inhibit uncompetitively or noncompetitively, but at high SP29-peptide-1 concentrations, inhibition tends to converge toward a common V_{max}, suggesting a competitive component (Figures 7C, 7D). This evidence for mixed inhibition with respect to SP29-peptide-1 suggests that 1-68A occupies parts of both donor and acceptor substrate sites.

Specificity of 1-68A and 2-68A

1-68A and 2-68A do not inhibit mammalian UDP-GlcNAc 4-epimerase, β4GalT1 (an inverting GT), or

Downloaded from https://academic.oup.com/glycob/article-abstract/15/5/489/602562 by Abdullah Gul Universitesi user on 02 April 2020

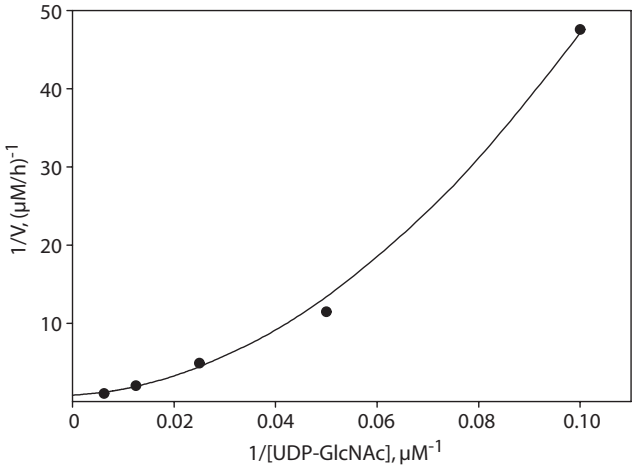


Fig. 4. Initial rate analysis of pp αGlcNAcT2 activity with respect to varying concentrations of SP29-peptide-1 and UDP-GlcNAc maintained at a fixed ratio of 1.0, replotted from Figure 2A. The curve represents the Haldane equation (Equation 3) based on experimental values and parameters derived from application of Equation 1 using parameters derived from Figures 2 and 3 (V_{max} = 1.3 mmole/h, $K_m^{UDP\text{-}GlcNAc}$ = 26 μM, $K_m^{SP29\text{-}peptide\text{-}1}$ = 28 μM), except that the $K_i^{UDP\text{-}GlcNAc}$ = 220 μM rather than the 190 μM value obtained before. R^2 = 0.997.

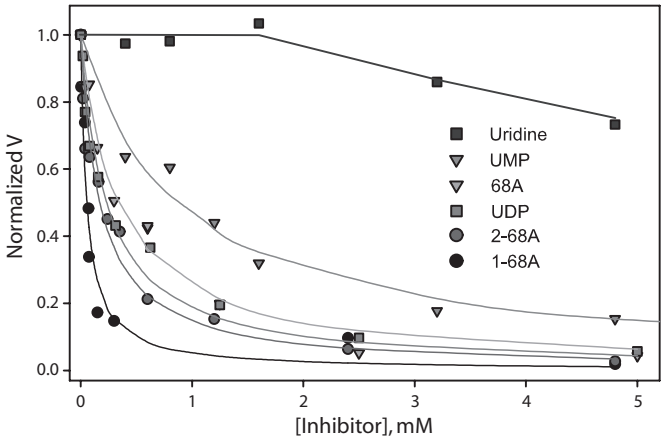


Fig. 5. Dose-dependent inhibition of pp αGlcNAcT2 initial rate by uridine derivatives. Reactions were incubated for 1 h in the presence of 38 μM UDP-GlcNAc, 0.3 mM SP29-peptide-1, and the indicated concentration of potential inhibitor as shown. Rates are normalized to values from reactions lacking the inhibitor. Data for each inhibitor (except uridine) are fitted to Equation 4 to model competitive inhibition.

α3GalT1 (a retaining GT) (Hang *et al*., 2004; Winans and Bertozzi, 2002). To address their specificity in *Dictyostelium*, two cytoplasmic retaining GTs that modify Skp1 were examined. pp αGlcNAcT1 is a polypeptide GT that modifies *Dictyostelium* Skp1 (van der Wel *et al*., 2002). 1-68A and 2-68A exerted only very weak inhibition of highly purified recombinant pp αGlcNAcT1 compared to their effects on pp αGlcNAcT2 (Figures 8A, 8B), despite similar susceptibility of both enzymes to inhibition by UDP (Figure 8C). Inhibition by 1-68A was competitive with respect to UDP-GlcNAc with an apparent K_i of 330 μM (data not shown). Although pp αGlcNAcT1 is in the same GT60 family as pp αGlcNAcT2 (Coutinho *et al*., 2003), its sequence is more phylogenetically distant (West *et al*., 2004), and the enzyme is distinct in its cytoplasmic localization and sub-μM apparent $K_m^{UDP\text{-}GlcNAc}$ value (Teng-umnuay *et al*., 1999; van der Wel *et al*., 2002), and therefore likely has a distinct active site architecture.

αGalT1 modifies the 3-OH position of Fuc, the third sugar residue on *Dictyostelium* Skp1, using UDP-Gal as the donor substrate (Ketcham *et al*., 2004). 1-68A at up to 300 μM failed to inhibit Skp1 αGalT1 (Figure 8A), assayed using a saturating concentration of Fucα1-pNP as the acceptor substrate, despite the sensitivity of the enzyme to UDP (Figure 8C). 2-68A exerted weak inhibition (Figure 8B), which was competitive with respect to UDP-GlcNAc with an apparent K_i of 300 μM (data not shown).

Although UDP inhibited all three enzymes similarly (Figure 8C), 1-68A and 2-68A were much more active against pp αGlcNAcT2, and the greater effect exerted by 1-68A relative to 2-68A on pp αGlcNAcT2 was not seen for the other two enzymes. Therefore the similar competitive inhibition by 1-68A and 2-68A on both the murine pp αGalNAcTs and *Dictyostelium* pp αGlcNAcT2, with apparent K_i values near to or below the K_m values for their sugar–nucleotide donor substrates, provides further support for a mechanistic similarity of these enzyme types.

Discussion

The kinetic analyses using a model synthetic peptide with multiple acceptor amino acids best support a compulsory ordered bi bi reaction mechanism for *Dd*-pp αGlcNAcT2. Double reciprocal plots of initial velocity as a function of one substrate concentration at varying fixed concentrations of the other substrate are linear (Figures 2, 3), and the data fit the expectation of the Haldane equation for this mechanism (Figure 4). The possibility that UDP-GlcNAc binds first is suggested by two results. First, substrate inhibition by SP85-peptide-2 (Figure 1A) is most consistent with its normally binding second as an acceptor substrate but at high concentration binding first and inhibiting the reaction. This effect has been observed for other enzymes that employ an ordered bi bi mechanism (Bheemanaik *et al*., 2003; Johnson-Winters *et al*., 2003; Kim *et al*., 2002). In addition, other enzymes utilizing substrates with high-energy phosphoester bonds, including the LgtC α4GalT from *Neisseria meningitidis* and creatine kinase, show structural changes on donor–substrate binding consistent with ordered binding (Lahiri *et al*., 2002; Persson *et al*., 2001). Second, compulsory binding of UDP-GlcNAc prior to the acceptor peptide is supported by the types of inhibition exerted by the donor substrate analog and product compound UDP with respect to UDP-GlcNAc (competitive) and SP29-peptide-1 (noncompetitive) (Table IX-6 in Segel, 1975). Initial binding of the sugar nucleotide is also seen in the retaining polypeptide GTs UDP-D-xylose:core protein α-xylosyltransferase (Kearns *et al*., 1991) and LgtC α4GalT (Persson *et al*., 2001).

Dd-pp αGlcNAcT2 exhibits a strong preference for UDP-GlcNAc relative to UDP-GalNAc, though it is not known if the latter can function at high concentrations. The enzyme modifies Ser at about two-thirds the rate of Thr in

Downloaded from https://academic.oup.com/glycob/article-abstract/15/5/489/602562 by Abdullah Gul Universitesi user on 02 April 2020

Table II. Inhibition type and estimated inhibition constants of uridine derivatives toward *Dd*-pp αGlcNAcT2

Varied substrate	Inhibitor	Figure	Inhibition pattern	Apparent K_i (μM)
UDP-GlcNAc	Uridine	5	None detected	> 2 mM
UDP-GlcNAc	UMP	6A	Competitive	140 ± 14
UDP-GlcNAc	UDP	6B	Competitive	89 ± 15
UDP-GlcNAc	UDP-GalNAc	Data not shown	Competitive	137 ± 63
UDP-GlcNAc	1-68A	6C	Competitive	35 ± 14
UDP-GlcNAc	2-68A	6D	Competitive	70 ± 14
UDP-GlcNAc	68A	6E	Competitive	220 ± 90
SP29 peptide-1	UDP	7B	Noncompetitive	440 ± 100

Inhibition pattern and apparent K_i values (± SEM) were derived from data shown in the figure indicated.

the same position in a separate peptide (Figure 1B), consistent with modification of Ser residues in vivo (Jung *et al.*, 1998). During the initial reaction there is a strong preference for modification of the five centrally located hydroxyamino acids of the 26-mer SP29-peptide-1 (Figure 1B, filled bars). Because the average of these reactions appears kinetically homogenous (Figure 1A, filled circles; Figure 3), it is likely that formation of the enzyme substrate complex is defined by a single K_m and that the positional profile of glycosylation reflects a stochastic distribution of hydroxyamino acids around the center of the peptide docking at the active site. Absence of modification near the N-terminus is consistent with previous data from SP85-peptide-2 (Wang *et al.*, 2003). The significance of the preference for central amino acids is not known because the peptides are contained within larger polypeptides in vivo. No evidence for processivity in the modification reaction was observed, consistent with the absence of the ricin-like domain that promotes preferential modification of previously glycosylated peptides in certain pp αGalNAcTs (Ten-Hagen *et al.*, 2003). Therefore it is likely that the studies shown here describe a family of single-hit reactions with similar kinetic parameters that favor the central region of the peptide but can modify peripheral residues.

Mm-pp αGalNAcT1, an example of the animal class of pp αGalNAcTs, appears to be related to *Dd*-pp αGlcNAcT2 based on distant sequence similarity of a 250-amino-acid region that corresponds to their catalytic domains (see *Introduction*). This similarity is supported by successful threading (unpublished data) of the *Dd*-pp αGlcNAcT2 sequence onto a just published structure of *Mm*-pp αGalNAcT1 (Fritz *et al.*, 2004). Kinetic analyses of *Mm*-pp αGalNAcT1, using an acceptor substrate (EPO-T) that contains only a single glycosylation site, suggested that the enzyme uses a random sequential bi bi mechanism (Wragg *et al.*, 1995). However, double reciprocal plots describing the dependence of initial rates of *Mm*-pp αGalNAcT1 on substrate concentrations, at fixed concentrations of the other substrate, yielded linear shapes more consistent with an ordered mechanism (Segel, 1975). In addition, UDP inhibition is competitive and noncompetitive with respect to UDP-GalNAc (nonsaturating concentration of EPO-T) and EPO-T (saturating UDP-GalNAc), respectively, which suggests that UDP-GalNAc is the first substrate to bind *Mm*-pp αGalNAcT1, based on comparison with other examples (Berrada *et al.*, 2002; Bheemanaik *et al.*, 2003; Evdokimov *et al.*, 2002; Kim *et al.*, 2002). In contrast, product inhibition in a random sequential bi bi mechanism is expected to have a noncompetitive or mixed-type pattern toward both substrates (Segel, 1975).

Using another approach (Wragg *et al.*, 1997), kinetic studies with a dead-end peptide analog inhibitor, EPO-G (in which the acceptor Thr residue was replaced by Gly), did not yield an uncompetitive inhibition pattern toward UDP-GalNAc characteristic an ordered mechanism (Segel, 1975). However, dead-end inhibitors can vary in their kinetic effects as seen for lipopolysaccharyl α-galactosyltransferase, MAP kinase kinase-2, and malic enzyme (Cleland, 1977; Ly *et al.*, 2002; Mallick *et al.*, 1990; Schindler *et al.*, 2002; Schimerlik and Cleland, 1977). For malic enzyme, which follows an ordered bi ter mechanism (similar to ordered bi bi), dead-end inhibitors (2-hydroxy acids) that are analogs of the second binding substrate (malate) exhibit noncompetitive (rather than uncompetitive) inhibition with respect to pyruvate in the direction of oxidation of TPNH. As suggested, this could occur if the 2-hydroxy acid binds the enzyme by mimicking the second substrate or related product in such a way that a hypothetical conformational change required for the reaction coordinate fails to occur, thereby locking the enzyme in an aberrant ternary complex and exerting a noncompetitive effect.

Further support for an ordered bi bi mechanism for *Mm*-pp αGalNAcT1 comes from inactivation studies that showed that it becomes more sensitive to inactivation by diethylpyrocarbonate in the presence of UDP-GalNAc but not in the presence of EPO-G. This suggests a physical interaction leading to a structural change prior to the binding of EPO-G, characteristic of the ordered mechanism. Furthermore, the absence of an effect of EPO-G on inactivation by diethylpyrocarbonate is consistent with no EPO-G binding without UDP-GalNAc. Therefore, the *Mm*-pp αGalNAcT1 data seem compatible with an ordered bi bi mechanism with initial binding of the sugar nucleotide, similar to the mechanism proposed for *Dd*-pp αGlcNAcT1. Nevertheless, additional approaches are required to rigorously establish how similar are the mechanisms of two enzyme classes. For comparison, galactokinase from different species varies in its mechanism

Downloaded from https://academic.oup.com/glycob/article-abstract/15/5/489/602562 by Abdullah Gul Universitesi user on 02 April 2020

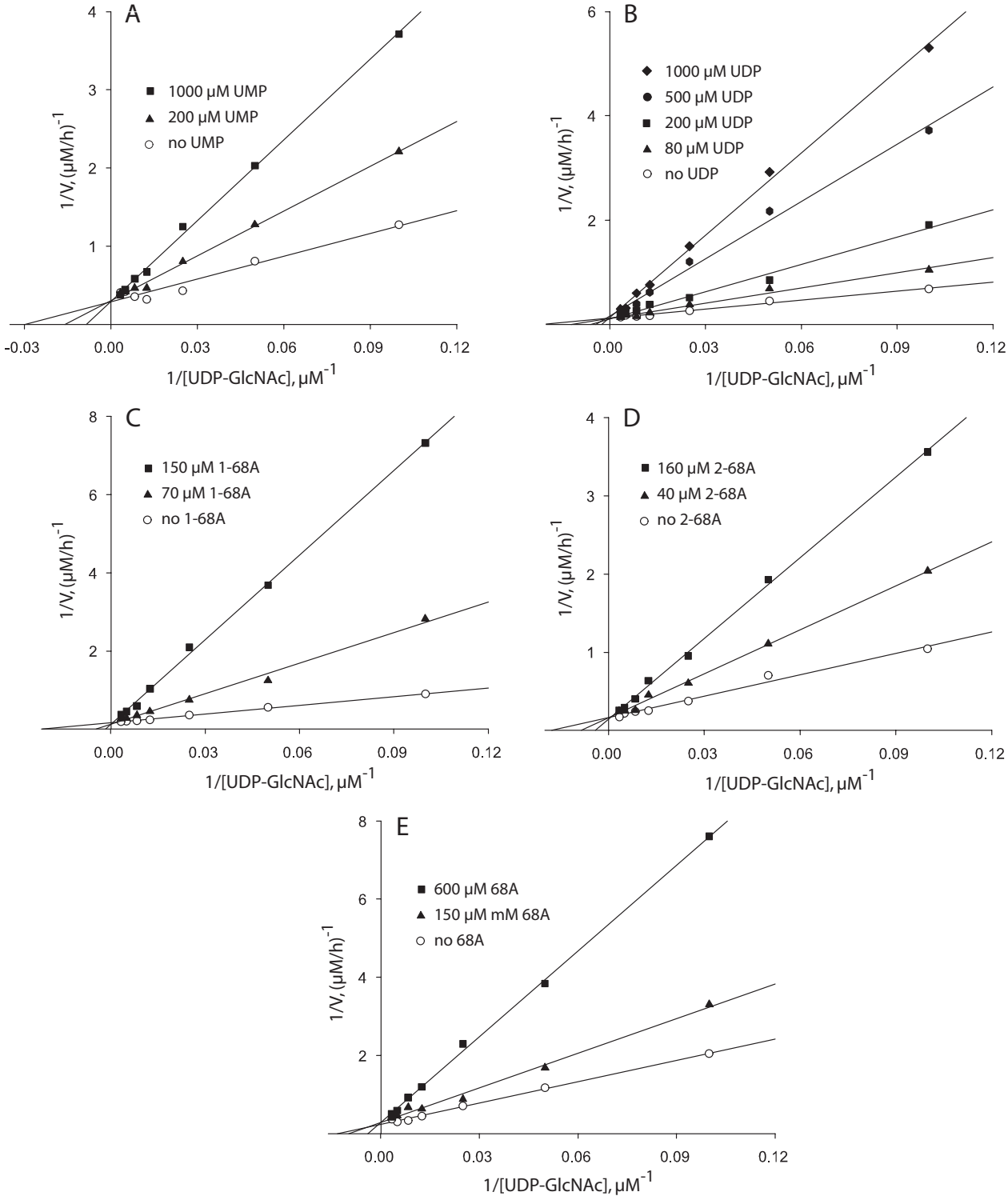


Fig. 6. Dependence of inhibition on donor substrate (UDP-GlcNAc) concentration. Double reciprocal plots of initial reaction rates of *Dd*-pp αGlcNAcT2 versus UDP-GlcNAc concentration in the presence of 400 μM SP29-peptide-1 and the indicated concentrations of (**A**) UMP, (**B**) UDP, (**C**) 1-68A, (**D**) 2-68A, or (**E**) 68A. Apparent K_i values derived from these data are summarized in Table II.

from random order of binding of its two substrates, to a compulsory order with either ATP first or galactose first (Holden *et al.*, 2003). In any case, both mechanisms are similar in the sense that they require binding of each substrate before chemical conversion and product release.

Like the pp αGalNAcTs, *Dd*-pp αGlcNAcT2 is susceptible to competitive inhibition with respect to the sugar–nucleotide substrate by uridine-based compounds. Although UDP is a good inhibitor, 1-68A and 2-68A are even better, with the former having an apparent K_i value similar to the apparent

Downloaded from https://academic.oup.com/glycob/article-abstract/15/5/489/602562 by Abdullah Gul Universitesi user on 02 April 2020

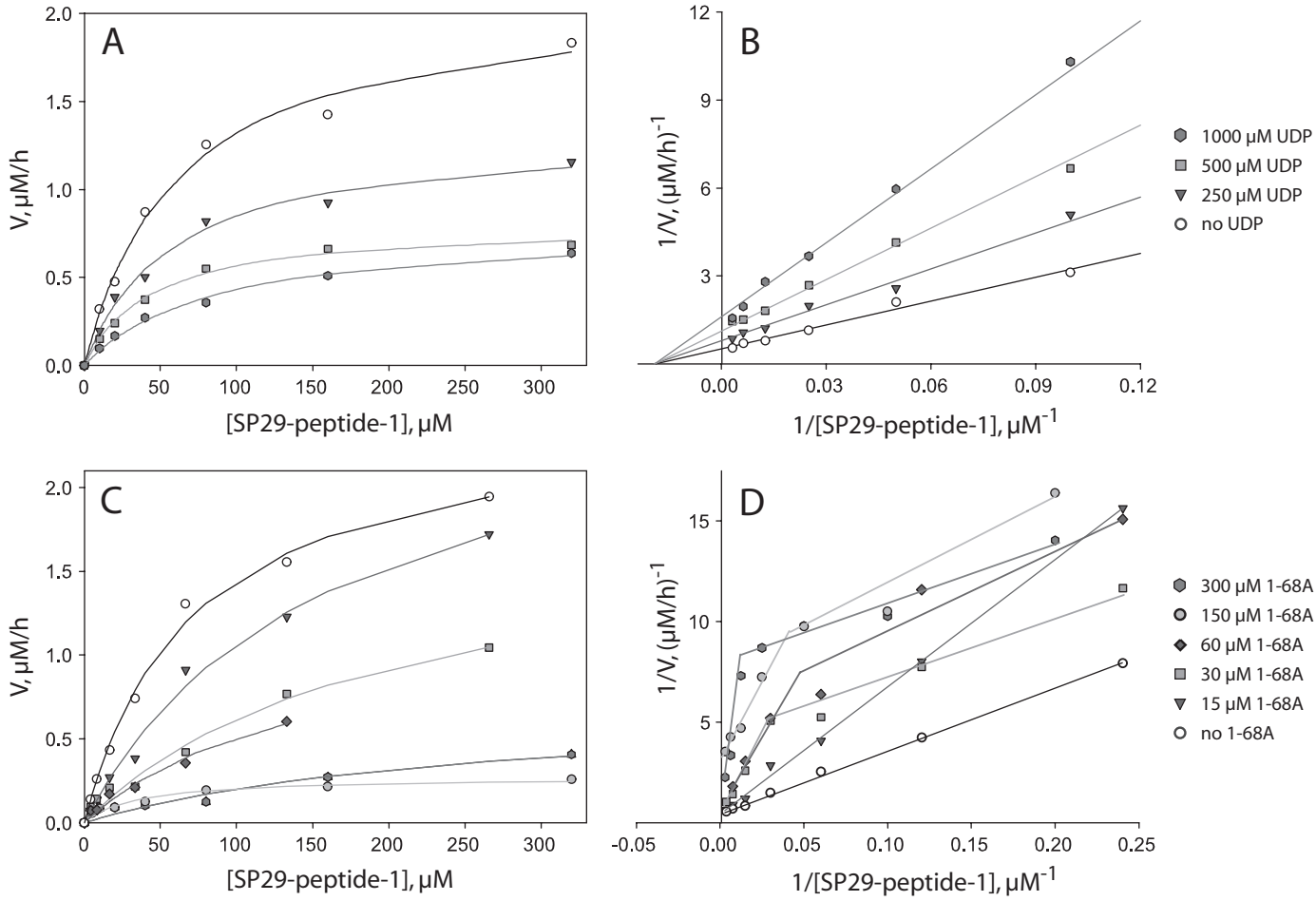


Fig. 7. Dependence of inhibition on acceptor substrate (SP29-peptide-1) concentration. Initial rates of *Dd*-pp αGlcNAcT2 were measured in the presence of 75 μM UDP-GlcNAc as a function of the SP29-peptide-1 concentration, at various concentrations of the inhibitors UDP (**A**, **B**) or 1-68A (**C**, **D**). Results are plotted in direct (**A**, **C**) and double reciprocal (**B**, **D**) fashion.

K_m value for UDP-GlcNAc (Figures 5–7; Table II). Inhibition by 1-68A and 2-68A was also affected by the SP29-peptide-1 concentration in a complex manner (Figures 7C, 7D) not reported for *Mm*-pp αGalNAcT1 (Hang *et al*., 2004). This effect, not observed for UDP (Figures 7A, 7B), suggests that the trihydroxybenzene moiety may interact with the acceptor substrate binding site on pp αGlcNAcT2. 1-68A and 2-68A inhibit murine pp αGalNAcTs similarly and competitively, with somewhat greater potencies than toward the *Dictyostelium* enzyme, and do not or only weakly inhibit other retaining GTs (Hang *et al*., 2004; Figure 8). The selectivity toward *Mm*-pp αGalNAcT1 and *Dd*-pp αGlcNAcT2 indicates that the enzyme active sites are related.

The similar kinetic properties of *Dd*-pp αGlcNAcT2 and *Mm*-pp αGalNAcT1 and their related susceptibility to uridine-based inhibitors supports the proposed common evolutionary origin based on sequence comparisons (Wang *et al*., 2003; West *et al*., 2004). The similarity appears to be functionally meaningful because mammalian MUC1 and MUC2 fragments expressed in *Dictyostelium* are *O*-glycosylated (probably by *Dd*-pp αGlcNAcT2; Wang *et al*., 2003) in a pattern similar to that found in the native proteins (Jung *et al*., 1998). Nevertheless, UDP-GalNAc is not a (or at best very poor) substrate for *Dd*-pp αGlcNAcT2, suggesting that the greatest difference between the two enzyme classes is in recognition of the donor sugar moiety. The original pp αGlcNAcTs may have converted to GalNAcTs when the specificity of the UDP-Gal epimerase broadened to include UDP-GalNAc (Roper and Ferguson, 2003). Because *Dd*-pp αGlcNAcT lacks the C-terminal ricin-like domain of the pp αGalNAcT family (Ten Hagen *et al*., 2003), this domain may not be essential for the core catalytic activity of these GTs.

1-68A and 2-68A appear to act on *Mm*-pp αGalNAcT1 in cultured cells (Hang *et al*., 2004). Therefore, these compounds may help in the development of inhibitors against the related pp αGlcNAcTs in trypanosomes and probably oomycete plant pathogens. The differential effects of 1-68A and 2-68A on *Dd*-pp αGlcNAcT2 and their mixed inhibition with respect to the acceptor substrate, not observed for *Mm*-pp αGalNAcT1, suggest that it will be possible to develop inhibitors specific for each enzyme type.

Materials and methods

Dd-*pp αGlcNAcT2*

A soluble recombinant form of *Dd*-pp αGlcNAcT2, in which its native N-terminal signal anchor is replaced by a

Downloaded from https://academic.oup.com/glycob/article-abstract/15/5/489/602562 by Abdullah Gul Universitesi user on 02 April 2020

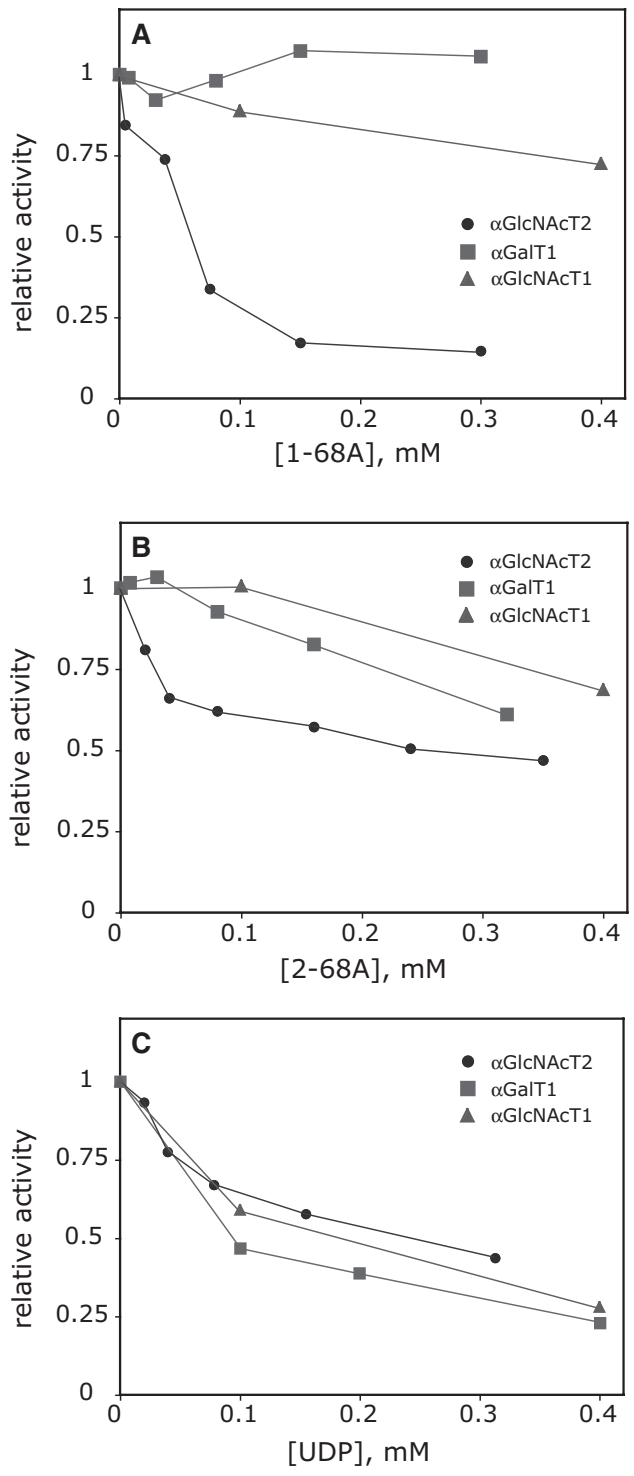


Fig. 8. Effects of uridine conjugates on other retaining GTs. Initial velocity measurements of *Dd*-αGalT1 (squares) were performed in the presence of 4 μM UDP-Gal, 8 μM Fucα1-pNP, and increasing concentrations of the indicated uridine derivative (**A**, 1-68A; **B**, 2-68A; **C**, UDP). Initial velocities of *Dd*-pp αGlcNAcT1 (triangles) were measured in the presence of 0.2 μM UDP-GlcNAc, an unsaturating concentration of Skp1A1-myc, and increasing concentrations of the indicated uridine derivative. The values for UDP are from Tengumnuay *et al.* (1999). Initial velocity measurements for pp αGlcNAcT2 (circles), in the presence of 50 μM UDP-GlcNAc, are from Figure 5. The UDP-sugar concentrations are near the K_m values for their respective enzymes.

cleavable signal peptide, was expressed and purified to near homogeneity from the culture medium of *Dictyostelium* as described (Wang *et al.*, 2003) and stored at −80°C. When thawed, aliquots were diluted 10-fold in an ice-cold buffer optimized for enzyme stability: 50 mM 2-(*N*-morpholino)ethanesulfonic acid–NaOH, pH 6.0, 0.1 mM dithiothreitol (DTT), 0.2% (v/v) Tween-80, and 5 mM $MnCl_2$.

Enzyme activity was measured based on transfer of radioactivity from UDP-[^{3}H]GlcNAc to a synthetic acceptor peptide. Unless otherwise indicated, this was SP29-peptide-1 (Table I), which encompasses the mucin-like domain of the cell-surface GPI-anchored glycoprotein SP29 (PsA) (Wang *et al.*, 2003). The 50-μl reaction volume contained 50 mM HEPES-NaOH, pH 7.5, 5 mM $MnCl_2$, 0.1% Tween 80, 0.1 mM DTT, 1 nM *Dd*-pp αGlcNAcT2, 10–400 μM SP29-peptide-1, and 10–500 μM UDP-GlcNAc, which included 1.7×10^6 dpm UDP-[6-^{3}H]GlcNAc (60 Ci/mmol; American Radiochemical, St. Louis, MO). The reaction was initiated by addition of pp αGlcNAcT2 in 5.0 μl, incubated at 29°C for 1.0 h, and terminated by addition of 1 ml 10 mM Na-EDTA, pH 8.0. Incorporation into peptide was determined by adsorption to a C_{18}-SepPak, washing with water, elution with MeOH, and liquid scintillation counting in the presence of BioSafe-II (Fisher, Silver Spring, MD) as described (Wang *et al.*, 2003). Incorporation was linear with respect to time under the conditions tested (data not shown). In a control experiment for selectivity, it was found that when the MeOH-eluted material was dried, redissolved in H_2O, and applied to a reconditioned C_{18}-SepPak, less than 3% of the dpm were found in the flow-through fraction.

In some trials, UDP-GlcNAc was replaced by UDP-[6-^{3}H]GalNAc (60 Ci/mmol; American Radiochemical).

Sequential Edman degradation of the reaction product

The product of a reaction containing 240 μM SP29-peptide-1 or -2 (0.1% modified) and 500 μM UDP-GlcNAc was adsorbed to a C_{18}-SepPak, eluted with 50% MeOH, dried in a vacuum centrifuge, and redissolved in 60% (v/v) solution A (3.5% [v/v] tetrahydrofuran, 3.6% [v/v] CH_3COOH, 0.3% [w/v] 1-heptane sulfonic acid, 0.4% [w/v] NaOH in H_2O) and 40% B (12% [v/v] isopropanol and 88% [v/v] acetonitrile). Samples (10,000 dpm, 150 pmol) were then subjected to standard Edman degradation in an Applied Biosystems (Foster City, CA) Procise 392 automated sequenator. The eluate from each cycle (1.5 ml) was counted for radioactivity as described. Raw dpm values for each cycle were corrected for loss based on 92% repetitive yield and lag owing to incomplete cleavage (60%) of Pro residues. Except for positions 1–4 (prior to the first Pro residue), dpm were allocated only to positions containing Thr or Ser.

Other GT enzymes

The activity of highly purified recombinant *Dd*-pp αGlcNAcT1 was assayed in the presence of 0.2 μM UDP-GlcNAc and a subsaturating concentration of a highly purified preparation of Skp1A1-myc from *Dictyostelium*, and incorporation measured using the sodium dodecyl sulfate–polyacrylamide gel electrophoresis assay as previously described (van der Wel *et al.*, 2002). Activity of partially purified UDP-Gal:fucoside αGalT1 was measured as described previ-

Downloaded from https://academic.oup.com/glycob/article-abstract/15/5/489/602562 by Abdullah Gul Universitesi user on 02 April 2020

ously using the C_{18}-SepPak assay to detect incorporation into Fucα1-pNP (Ketcham *et al.*, 2004). Initial velocities were determined in the presence of 4 μM UDP-Gal (containing 0.25 μM UDP-[6-^{3}H]Gal, 20 Ci/mmol) and 8 mM Fucα1-pNP.

Kinetic analyses

Kinetic parameters were initially estimated by fitting to Equation 1 (Segel, 1975) using a nonlinear regression method in SigmaPlot 8.0 (Marquardt-Levenberg algorithm).

$$V = V_{max}[S]/([S] + K_m) \quad (1)$$

In the case of the acceptor substrate SP85-peptide-2 (Table I), which appeared to inhibit at higher concentrations, parameters were estimated by fitting data to Equation 2 (Segel, 1975) using nonlinear regression as before.

$$v = V_{max}[S]/(K_m + [S] + ([S]^2 / K_i)) \quad (2)$$

K_i represents the dissociation constant for inhibitory binding of the substrate.

To investigate the reaction mechanism, UDP-GlcNAc was varied from 10 to 300 μM at different fixed concentrations of SP29-peptide-1 from 10 to 320 μM. Based on the appearance of double reciprocal plots of the data (see *Results*), kinetic parameters were determined for an ordered bi bi mechanism based on graphical analyses of double reciprocal plots of the data (Segel, 1975), as shown in Figures 2 and 3.

The data were also fitted to the Haldane equation (Equation 3), where initial velocity is plotted as a function of varying equal concentrations of both substrates (A) (Segel, 1975). Based on the following values (from Figures 2, 3), X = [A]/[B] = 1; V_{max} = 1.3 μM/h, K_m^A = 26 μM, and K_m^B = 28 μM, the data were fitted best using nonlinear regression as previously by a K_i^A value of 220 ± 5 μM.

$$1/V = [K_m^A/[A]V_{max}\,(1 + K_i^A K_m^B/xK_m^A[A] + K_m^B/xK_m^A)] + 1/V_{max} \quad (3)$$

Inhibitor studies and data analysis

Effects of potential inhibitors were tested using the standard reaction described, which usually contained 50 μM UDP-GlcNAc and 400 μM SP29-peptide-1. Initial rates were normalized by dividing by the corresponding rate in the absence of inhibitor. Normalized rates (a) were modeled by Equation 4 (Segel, 1975) for competitive inhibition using nonlinear regression as before.

$$a = ([S] + K_m)/([S] + K_m(1 + [I]/K_i)) \quad (4)$$

S, I, K_m, and K_i are the concentration of substrate whose level is varied, inhibitor concentration, Michaelis-Menten constant, and dissociation constant of the inhibitor, respectively. The other substrate was at a saturating level (200–400 μM). Apparent K_i values were averaged from values obtained at different inhibitor concentrations and are reported as ± SEM.

Based on the appearance of the double reciprocal plots (see *Results*), inhibition data were fitted to Equation 5 for pure competitive inhibition or Equation 6 for noncompetitive inhibition (Segel, 1975), using nonlinear regression as before.

$$V = V_{max}[S]/([S] + K_m(1 + [I]/K_i)) \quad (5)$$

$$V = V_{max}[S]/[(1 + [I]/K_i)(K_m + [S])] \quad (6)$$

V and V_{max} represent the rate at any substrate concentration and maximum rate at the saturated substrate concentrations, respectively.

Acknowledgments

We are grateful to Howard C. Hang and Carolyn R. Bertozzi (Berkeley) for their generous gift of the 1-68A, 2-68A, and 68A compounds and discussions; Fei Wang for purified *Dd*-pp αGlcNAcT2; and the OUHSC Molecular Biology Resource Facility for the Edman degradation analyses. This work was supported by NIH grant R01-GM37539 and NSF grant MCB-0240634.

Abbreviations

DTT, dithiothreitol; GPI, glycosylphosphatidylinositol; GT, glycosyltransferase; pp, polypeptide.

References

Berrada, W., Naya, A., Iddar, A., and Bourhim, N. (2002) Purification and characterization of cytosolic glycerol-3-phosphate dehydrogenase from skeletal muscle of jerboa (*Jaculus orientalis*) *Mol. Cell. Biochem.*, **231**, 117–127.

Bheemanaik, S., Chandrashekaran, S., Nagaraja, V., and Rao, D.N. (2003) Kinetic and catalytic properties of dimeric *Kpn*I DNA methyltransferase. *J. Biol. Chem.*, **278**, 7863–7874.

Burleigh, B.A. and Andrews, N.W. (1998) Signaling and host cell invasion by *Trypanosoma cruzi*. *Curr. Opin. Microbiol.*, **1**, 461–465.

Cleland, W.W. (1977) Determining the chemical mechanisms of enzyme-catalyzed reactions by kinetic studies. *Adv. Enzymol.*, **45**, 273–387.

Coutinho, P.M., Deleury, E., Davies, G.J., and Henrissat, B. (2003) An evolving hierarchical family classification for glycosyltransferases. *J. Mol. Biol.*, **328**, 307–317.

Evdokimov, A.A., Zinoviev, V.V., Malygin, E.G., Schlagman, S.L., and Hattman, S. (2002) Bacteriophage T4 Dam DNA-[N-6-adenine]methyltransferase—kinetic evidence for a catalytically essential conformational change in the ternary complex. *J. Biol. Chem.*, **277**, 279–286.

Fritz, T.A., Hurley, J.H., Trinh, L.B., Shiloach, J., and Tabak, L.A. (2004) The beginnings of mucin biosynthesis: the crystal structure of UDP-GalNAc:polypeptide alpha-N-acetylgalactosaminyltransferase-T1. *Proc. Natl Acad. Sci. USA*, **101**, 15307–15312.

Hagen, F.K., Hazes, B., Raffo, R., deSa, D., and Tabak, L.A. (1999) Structure-function analysis of the UDP-*N*-acetyl-D-galactosamine:polypeptide *N*-acetylgalactosaminyltransferase. *J. Biol. Chem.*, **274**, 6797–6803.

Hang, H.C., Yu, C., Ten Hagen, K.G., Tian, E., Winans, K.A., Tabak, L.A., and Bertozzi, C.R. (2004) Small molecule inhibitors of mucin-type *O*-linked glycosylation from a uridine-based library. *Chem. Biol.*, **11**, 337–345.

Holden, H.M., Rayment, I., and Thoden, J.B. (2003) Structure and function of enzymes of the Leloir pathway for galactose metabolism. *J. Biol. Chem.*, **278**, 43885–43888.

Johnson-Winters, K., Purpero, V.M., Kavana, M., Nelson, T., and Moran, G.R. (2003) (4-Hydroxyphenyl)pyruvate dioxygenase from

Downloaded from https://academic.oup.com/glycob/article-abstract/15/5/489/602562 by Abdullah Gul Universitesi user on 02 April 2020

Streptomyces avermitilis: the basis for ordered substrate addition. *Biochemistry*, **42**, 2072–2080.

Jung, E., Gooley, A.A., Packer, N.H., Karuso, P., and Williams, K.L. (1998) Rules for the addition of *O*-linked N-acetylglucosamine to secreted proteins in *Dictyostelium discoideum*—in vivo studies on glycosylation of mucin MUC1 and MUC2 repeats. *Eur. J. Biochem.*, **253**, 517–524.

Kearns, A.E., Campbell, S.C., Westly, J., and Schwartz, N.B. (1991) Initiation of chondroitin sulfate biosynthesis: a kinetic analysis of UDP-D-Xylose:core protein α-D-xylosyltransferase. *Biochemistry*, **30**, 7477–7483.

Ketcham, C., Wang, F., Fisher, S.Z., Ercan, A., van der Wel, H., Locke, R.D., Sirajud-Doulah, S., Matta, K.L., and West, C.M. (2004) Specificity of a soluble UDP-galactose:fucoside α1,3galactosyltransferase that modifies the cytoplasmic glycoprotein Skp1 in *Dictyostelium. J. Biol. Chem.*, **279**, 29050–29059.

Kim, Y.-K., Kitaoka, M., Krishnareddy, M., Mori, Y., and Hayashi, K. (2002) Kinetic studies of a recombinant cellobiose phosphorylase (CBP) of the *Clostridium thermocellum* YM4 strain expressed in *Escherichia coli. J. Biochem.*, **132**, 197–203.

Lahiri, S.D., Wang, P.F., Babbitt, P.C., McLeish, M.J., Kenyon, G.L., and Allen, K.N. (2002) The 2.1 Å structure of *Torpedo californica* creatine kinase complexed with the ADP-Mg^{2+}-NO_3-creatine transition-state analogue complex. *Biochemistry*, **41**, 13861–13867.

Ly, H.D., Lougheed, B., Wakarchuk, W.W., and Withers, S.G. (2002) Mechanistic studies of a retaining a-galactosyltransferase from *Neisseria meningitidis*. *Biochemistry*, **41**, 5075–5085.

Mallick, S., Harris, B.G., and Cook, P.F. (1990) Kinetic mechanism of NAD:malic enzyme from *Ascaris suum* in the direction of reductive carboxylation. *J. Biol. Chem.*, **266**, 2732–2738.

O'Connor, R.M., Kim, K., Khan, F., and Ward, H.D. (2003) Expression of Cpgp40/15 in *Toxoplasma gondii*: a surrogate system for the study of *Cryptosporidium* glycoprotein antigens. *Infect. Immun.*, **71**, 6027–6034.

Perez-Vilar, J. and Hill, R.L. (1999) The structure and assembly of secreted mucins. *J. Biol. Chem.*, **274**, 31751–31754.

Persson, K., Ly, H.D., Dieckelmann, M., Wakarchuk, W.W., Withers, S.G., and Strynadka, N.C.J. (2001) Crystal structure of the retaining galactosyltransferase LgtC from *Neisseria meningitidis* in complex with donor and acceptor sugar analogs. *Nature Struct. Biol.*, **8**, 166–175.

Previato, J.O., Sola-Penna, M., Agrellos, O.A., Jones, C., Oeltmann, T., Travassos, L.R., and Mendonça-Previato, L. (1998) Biosynthesis of *O*-*N*-acetylglucosamine-linked glycans in *Trypanosoma cruzi*. Characterization of the novel uridine diphospho-*N*-acetylglucosamine:polypeptide *N*-acetylglucosaminyltransferase-catalyzing formation of *N*-acetylglucosamine-alpha1–>O-threonine. *J. Biol. Chem.*, **273**, 14982–14988.

Roper, J.R. and Ferguson, M.A. (2003) Cloning and characterisation of the UDP-glucose 4′-epimerase of *Trypanosoma cruzi*. *Mol. Biochem. Parasitol.*, **132**, 47–53.

Schimerlik, M.I. and Cleland, W.W. (1977) Inhibition and alternate-substrate studies on the mechanism of malic enzyme. *Biochemistry*, **16**, 565–570.

Schindler, J.F., Godbey, A., Hood, W.F., Bolten, S.L., Broadus, R.M., Kasten, T.P., Cassely, A.J., Hirsch, J.F., Merwood, M.A., Nagy, M.A., and others. (2002) Examination of the kinetic mechanism of mitogen-activated protein kinase activated protein kinase-2. *Biochim. Biophys. Acta*, **1598**, 88–97.

Schwientek, T., Bennet, E.P., Flores, C., Thacker, J., Hollmann, M., Reis, C.A., Behrens, J., Mandel, U., Keck, B., Schafer, M.A., and others. (2002) Functional conservation of subfamilies of putative UDP-N-acetylgalactosamine:polypeptide N-acetylgalactosaminyltransferases in *Drosophila*, *Caenorhabditis elegans*, and mammals. *J. Biol. Chem.*, **277**, 22623–22638.

Segel, I.H. (1975) *Enzyme kinetics*. John Wiley and Sons, New York.

Spiro, R.G. (2002) Protein glycosylation: nature, distribution, enzymatic formation, and disease implications of glycopeptide bonds. *Glycobiology*, **12**, 43R–56R.

Teng-umnuay, P., van der Wel, H., and West, C.M. (1999) Identification of a UDP-GlcNAc:Skp1-Hydroxyproline GlcNAc-transferase in the cytoplasm of *Dictyostelium*. *J. Biol. Chem.*, **274**, 36392–36402.

Ten Hagen, K.G. and Tran, D.T. (2002) A UDP-GalNAc:polypeptide N-acetylgalactosaminyltransferase is essential for viability in *Drosophila melanogaster*. *J. Biol. Chem.*, **277**, 22616–22622.

Ten Hagen, K.G., Fritz, T.A., and Tabak, L.A. (2003) All in the family: the UDP-GalNAc:polypeptide N-acetylgalactosaminyltransferases. *Glycobiology*, **13**, 1–16.

van der Wel, H., Morris, H., Panico, M., Paxton, T., Dell, A., Kaplan, L., and West, C.M. (2002) Molecular cloning and expression of a UDP-GlcNAc:hydroxyproline polypeptide GlcNAc-transferase that modifies Skp1 in the cytoplasm of *Dictyostelium*. *J. Biol. Chem.*, **277**, 46328–46337.

Varki, A. (1993) Biological roles of oligosaccharides: all of the theories are correct. *Glycobiology*, **3**, 97–130.

Varki, A., Cummings, R., Esko, J., Freeze, H., Hart, G., and Marth, J., eds. (1999) *Essentials of glycobiology*. Cold Spring Harbor Laboratory Press, New York, pp. 171–182.

Wang, F., Metcalf, T., van der Wel, H., and West, C.M. (2003) Initiation of mucin-type *O*-glycosylation in *Dictyostelium* is homologous to the corresponding step in animals and is important for spore coat function. *J. Biol. Chem.*, **278**, 51395–51407.

West, C.M. (2003) Comparative analysis of spore coat formation, structure and function in *Dictyostelium*. *Int. Rev. Cyt.*, **222**, 237–293.

West, C.M., van der Wel, H. Sassi, S., and Gaucher, E.A. (2004) Cytoplasmic glycosylation of protein-hydroxyproline and its relationship to other glycosylation pathways. *Biochim. Biophys. Acta*, **1673**, 29–44.

Winans, K.A. and Bertozzi, C.R. (2002) An inhibitor of the human UDP-GlcNAc 4-epimerase identified from a uridine-based library: a strategy to inhibit *O*-linked glycosylation. *Chem. Biol.*, **9**, 113–129.

Wojczyk, B.S., Stworka-Wojczyk, M.M., Hagen, F.K., Striepen, B., Hang, H.C., Bertozzi, C.R., Roos, D.S., and Spitalnik, S.L. (2003) cDNA cloning and expression of UDP-N-acetyl-D-galactosamine: polypeptide N-acetylgalactosaminyltransferase T1 from *Toxoplasma gondii*. *Mol. Biochem. Parasitol.*, **131**, 93–107.

Wragg, S.W., Hagen, F.K., and Tabak, L.A. (1995) Kinetic analysis of a recombinant UDP-*N*-acetyl-D-galactosamine:polypeptide *N*-acetylgalactosaminyltransferase. *J. Biol. Chem.*, **270**, 16947–16954.

Wragg, S.W., Hagen, F.K., and Tabak, L.A. (1997) Identification of essential histidine residues in UDP-N-acetyl-D-galactosamine:polypeptide *N*-acetylgalactosaminyltransferase-T1. *Biochem. J.*, **328**, 193–197.

Zachara, N.E., Packer, N.H., Temple, M.D., Slade, M.B., Jardine, D.R., Karuso, P., Moss, C.J., Mabbutt, B.C., Curmi, P.M.G., Williams, K.L., and Gooley, A.A. (1996) Recombinant prespore-specific antigen from *Dictyostelium discoideum* is a β-sheet glycoprotein with a spacer peptide modified by *O*-linked N-acetylglucosamine. *Eur. J. Biochem.*, **238**, 511–518.

Downloaded from https://academic.oup.com/glycob/article-abstract/15/5/489/602562 by Abdullah Gul Universitesi user on 02 April 2020